Engineered Science

RESEARCH PAPER

View Article Online

Interfacial and Glass Transition Properties of Surface-Treated Carbon Fiber Reinforced Polymer Composites under Hygrothermal Conditions

Bin Yu,[1] Xiaotuo Li,[1] Jinliang An,[2] Zhenyu Jiang*[3] and Jinglei Yang*[4]

Carbon fiber reinforced polymer (CFRP) composites have attracted considerable attention because of their high specific mechanical properties. A promising application of CFRP is in marine and offshore area, where the satisfactory long-term performance of the composite is highly dependent on the interlaminar properties and matrix degradation due to moisture intake. This paper presents a systematic study of how moisture absorption and fiber surface treatment affect the interfacial properties of CFRP. A well-defined and characterised treating method combing silane coupling agent together with multiwalled carbon nanotubes (MWCNTs) is used to modify carbon fiber surfaces. Carbon/epoxy laminates were fabricated using vacuum assisted resin transfer moulding method and then placed in hygrothermal environment at 80 °C for 60 days. Mode I and Mode II interlaminar fracture toughness and interlaminar shear strength (ILSS) were evaluated through double cantilever beam (DCB) tests, end-notch flexure tests (ENF) and short beam shear (SBS) tests, respectively. The obtained results show that ILSS, mode I and mode II interlaminar fracture toughness, and glass transition temperature (Tg) of laminates decrease after enduring the hygrothermal aging. It is found that silane treatment can improve the interlaminar fracture toughness of laminates, and incorporation of MWCNTs can further enhance these interfacial properties. The average values of mode I and II fracture toughness and interlaminar shear strength of the laminates are 33%, 40.5% and 4.3% higher than the untreated samples after hygrothermal aging, respectively. However, surface treatment shows insignificant effect on Tg of composite laminates, probably because these properties were mainly dominated by epoxy matrix.

Keywords: Carbon fibers; Carbon nanotubes; Hygrothermal effect; Fracture toughness; Interfacial strength

Received 24th April 2018, Accepted 7th May 2018

DOI: 10.30919/es8d628

1. Introduction

Carbon fiber reinforced polymer (CFRP) composites have found increasing applications in marine and offshore area recently because of their superior specific mechanical properties. For safety and long term working efficiency, their resistance to environmental exposure attracts much attention.[1] As moisture and heat may degrade the mechanical properties of CFRP, especially which are related to fiber-matrix interface, it is of great importance to investigate the hygrothermal effects on CFRP and improve the interfacial resistance of composites to environment.

To improve fiber matrix bonding strength, many methods were developed to modify both carbon fibers and matrix, such as fiber sizing and coating, electrochemical oxidation, liquid-phase chemical oxidation and incorporating nanofillers into matrix directly.[2–5] A new method emerged very recently that sizing doped with nanofillers can be applied onto carbon fibers to enhance the interphase between carbon fibers and matrix.[6–9]

Moisture is unfriendly to CFRPs, impairing the bonding between polymer matrix and fibers. Complete immersion in water constitutes the most sever environment, which unfortunately is the real condition where offshore structures work. The effects of water on the interfacial properties of CFRP can manifest themselves more quickly when the moisture diffusion rates is accelerated under high temperature.[10–17]

In this paper, MWCNTs were dispersed in silane coupling agent and then the solution was applied to the carbon fiber cloth. The hygrothermal effects on different treated CFRP composites were compared. The Mode I and Mode II interlaminar fracture toughness and interlaminar shear strength of CFRP were evaluated using double cantilever beam (DCB) tests, end-notch flexure tests (ENF) and short beam shear (SBS) tests, respectively. The reinforcement mechanisms were analysed according to the characterization of fractured surface morphology and glass transition temperature variation.

[1] *School of Mechanical and Aerospace Engineering, Nanyang Technological University, Singapore, 639798*
[2] *School of Materials and Energy, University of Electric Science and Technology, Chengdu 611731, China*
[3] *School of Civil Engineering and Transportation, South China University of Technology, Guangzhou 510640, China. E-mail: zhenyujiang@scut.edu.cn*
[4] *Department of Mechanical and Aerospace Engineering, Hong Kong University of Science and Technology, Hong Kong, SAR, China. E-mail: maeyang@ust.hk*

2. Experimental

2.1. materials

The composite laminates were prepared using commercially available HexTow IM2C carbon fibre cloth in a 2-2 twill configuration as the primary reinforcement. Multiwalled carbon nanotubes used as secondary reinforcement were Nanocyl NC7000. The epoxy matrix, Epolam 5015 resin, is a mixture of Bisphenol F and Bisphenol A resins supplied by Axson Technologies. The Epolam 5015 hardener consists of isophoronediamine and polyoxypropylenediamine. (3-glycidyloxypropyl) trimethoxysilane coupling agent was obtained from Sigma-Aldrich.

2.2. Preparation of coating

The preparation of coating solution and working mechanism of silane coupling agent has been discussed in detail in previous paper.[18] A mixture of ethanol and water with ratio of 95:5 was prepared and PH value was adjusted to 5. (3-glycidyloxypropyl) trimethoxysilane was then added into the solvent to yield a 2% final concentration. The introduction of MWCNTs with loading of 0.05 wt% into the solution was achieved by ultrasonicating for 30 minutes and then followed the same procedure. After the solution has been prepared, the carbon fiber cloth sheets were then soaked in the silane coupling agent solution (with or without MWCNTs) for several minutes followed by drying at 110°C for 20 minutes. For easier discussion, the composites with as received carbon fibers, silane coupling agent treated carbon fibers and CNTs modified silane treated carbon fibers are defined as CF, SL-CF and CNT/SL-CF, respectively.

2.3. CFRP laminates preparation

The carbon-epoxy composites were manufactured using Vacuum Assisted Resin Transfer Moulding (VARTM) process. The composites were created using 8 layers of carbon fiber sheets with a layer of Teflon film placed in between the 4th and 5th layer in the Mode I and Mode II fracture toughness samples to introduce a preliminary crack. Peel-ply was added above these layers and finally an infusion mesh was added on top of the peel-ply to aid the wet out of the fibers. The epoxy resin was fed into the vacuum bag with a polyvinyl chloride hose and infusion spiral until fully distributed within the layers. This set up can be seen in Fig. 1a and b. The laminate was left to cure at room temperature for 24 hours and then post cured at 80°C for 16 hours. The average thickness of the samples was measuring around 3.0 mm.

2.4. Moisture conditioning

The effect of moisture absorption on the mechanical properties of each treated composite was observed by submerging each type of composite specimen in tap water held at 80°C in a PolyScience 8305 circulating water bath for intervals of 10, 20, 30 and 60 days. At these pre-set moments, three specimens were removed from the bath, surface-dried to allow stable weights could be obtained. The weights were recorded using an electronic balance with a precision of ±0.005 mg and the weight gain was evaluated as a percentage of the original composite specimen weight using the following equation:

$$\text{Moisture content} = \frac{W_f - W_i}{W_i} \times 100\% \quad (1)$$

where W_i and W_f are the initial weight of the samples before water absorption and final weight of the samples after water absorption, respectively.

2.5. Characterization and mechanical tests

The surface topography of fractured specimens was characterized by field emission scanning electron microscope (FESEM, JEOL JSM 6700F). The glass transition temperature of epoxy matrix was verified by dynamic mechanical analysis (DMA), which was conducted on TADMA Q800 dynamic mechanical analyzer in single cantilever mode. The multi-frequency strain tests were run for three samples at amplitude of 15 μm and frequency of 1 Hz, with air Poisson's ratio of 0.3. The temperature was recorded between 30°C and 150°C. From the measurements of DMA tests, the temperature at which the

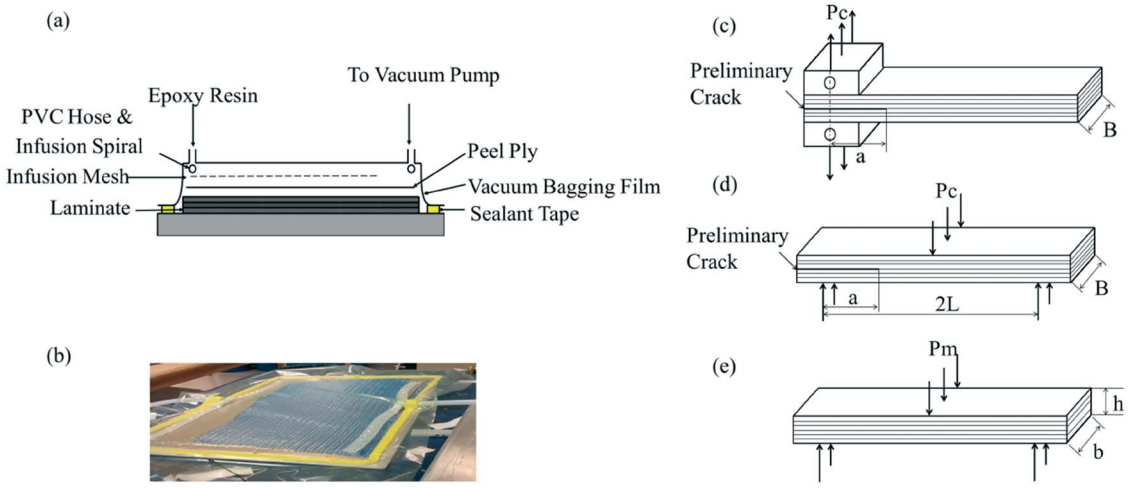

Fig. 1 (a) Schematic illustration of VARTM procedure; (b) Actual fabrication of CFRP composites using the VARTM process; Illustration of sample for: (c) Mode I interlaminar fracture toughness test; (d) Mode II interlaminar fracture toughness test; (e) Interlaminar shear strength test.

tanδ curve shows a maximum peak is recorded as the glass transition temperature (T_g) for the composites specimen. To achieve a comprehensive assessment of the interlaminar performance of the prepared composite laminates, three standard mechanical tests were carried out in this study, as elucidated below.

2.5.1. Mode I interlaminar fracture toughness. The Mode I interlaminar fracture toughness of the samples was determined in accordance with the ASTM D5528-01. The dimension of composite laminates for DCB tests was 157.5 mm × 25 mm with the starter crack length of 57.5 mm. To prepare the samples for loading, the edges of the samples were coated with a thin layer of water-based correction fluid ahead of the insert and vertical lines were drawn every 1 mm in order to aid the visualization of crack propagation. The double cantilever beam test was performed using Instron 5569 universal testing machine at crosshead speed of 2 mm/min. The sample is illustrated in Fig. 1c, and four samples are prepared for each composite. The modified beam compliance theory was used to calculate Mode I interlaminar fracture toughness using the following equation:

$$G_{IC} = \frac{3P_c\delta_c}{2B\left(a+\Delta\right)} \tag{2}$$

where G_{IC} is the Mode I interlaminar fracture toughness, P_c is the critical loading value, δ_c is the deflection value, B is the specimen width and a is the crack length, Δ is correction factor to account for rotation of the DCB arms. It is determined experimentally by generating a least squares plot of the cube root of compliance ($C^{1/3}$) as a function of delamination length, where C is δ_c/P_c.

The crack initiation value of $G_{IC(init)}$ is defined using the load and deflection measured at the point at which delamination is visually observed on the edge.

2.5.2. Mode II interlaminar fracture toughness. The dimension of composite laminates for ENF tests was 70 mm × 10 mm with the starter crack length of 20 mm and the effective span length of 60 mm. To determine the Mode II interlaminar fracture toughness (G_{IIC}) of the samples, an ENF test was performed using an Instron 5569 universal testing machine with crosshead speed of 2 mm/min at room temperature. The sample is illustrated in Fig. 1d, and eight samples are prepared for each composite. The Mode II interlaminar fracture toughness was determined for each specimen using the following equation:[19]

$$G_{IIC} = \frac{9a^2P_c\delta_c}{2B\left(2L^3+3a^3\right)} \tag{3}$$

where a is the crack length, P_c is the critical loading value, δ_c is the specimen deflection value, B is the specimen width and L is half of the span length. $G_{IIC(init)}$ values are obtained in a similar way mentioned in the previous subsection.

2.5.3. Interlaminar shear strength. Interlaminar Shear Strength (ILSS) of the samples was determined in accordance with the ASTM D2344/D2344M–00 standard using three-point short beam shear test. Dimension of composite laminates for SBS tests was 18 mm × 9 mm in size. The test was performed using an Instron 5569 universal testing machine at a crosshead speed of 2 mm/min. The sample is illustrated in Fig. 1e, and four samples are prepared for each composite. The ILSS values were determined using the following equation:

$$ILSS = 0.75 \times \frac{P_m}{b \times h} \tag{4}$$

where P_m is the maximum load, b is the specimen width and h is the specimen thickness.

3. Results and discussion

3.1. Water absorption

Water absorption tests were run for each kind of composite and the average moisture content calculated using Eq. (1) are listed in Fig. 2a. Water can be absorbed by composites through three ways:[20] firstly, water molecular diffuses into epoxy matrix directly; secondly, water flows along the interface between carbon fiber and epoxy matrix due to capillary effect; thirdly, water can exist in the loose area such as holes and microcracks. Results show that silane treated composite laminates absorbed more water with increasing the immersion time than the specimens with as-received carbon fibers, probably because the silane coating is hydrophilic and a kind of oligomer, which is looser compared with the cured epoxy matrix. Water can diffuse easily into the silane coating besides into the epoxy matrix. As a result, the SL-CF composites absorb more water than CF samples. When CNTs are dispersed into the silane coupling agent, the weight increase is even higher than silane treated samples due to the interfaces generated between CNTs and silane or epoxy matrix, which serve as routes for water uptake. In addition, because CNTs are oxidized, the presence of hydrophilic groups on the surface of CNTs can also lead to higher water absorption. For all the specimens, the weights were still increasing after 60-day immersion and more time was still needed to reach the saturation point.

3.2. DMA tests

Dynamic mechanical analysis was employed to determine the glass transition temperature of the samples by assessment of the tan δ vs. temperature curve peak, as shown in Fig. 2b. The glass transition temperatures of all three different treated composites are shown to decrease with increasing exposure time, implying that the polymeric matrixes of the composites are less likely to maintain their shape and strength after prolonged submersion in water as suggested by Odegard and Bandyopadhyay.[21] In fact, the absorbed water acts as an internal lubricant in the epoxy matrix, which decreases the energy barrier for chain segment movements of polymer.[20,22] In addition, small amounts of water can destroy the hydrogen bonds in epoxy matrix and cause decreases of T_g.[23,24] The results of each kind of composite are quite similar. This small variation in T_g of each composite confirms the dominance of matrix properties in glass transition of CFRPs.

3.3. Mode I interlaminar fracture toughness

The mode I fracture toughness was evaluated using Eq. (2) at each water exposure interval. Fig. 3a shows typical load-displacement curves for three composite systems (CF, SL-CF, CNT/SL-CF). The

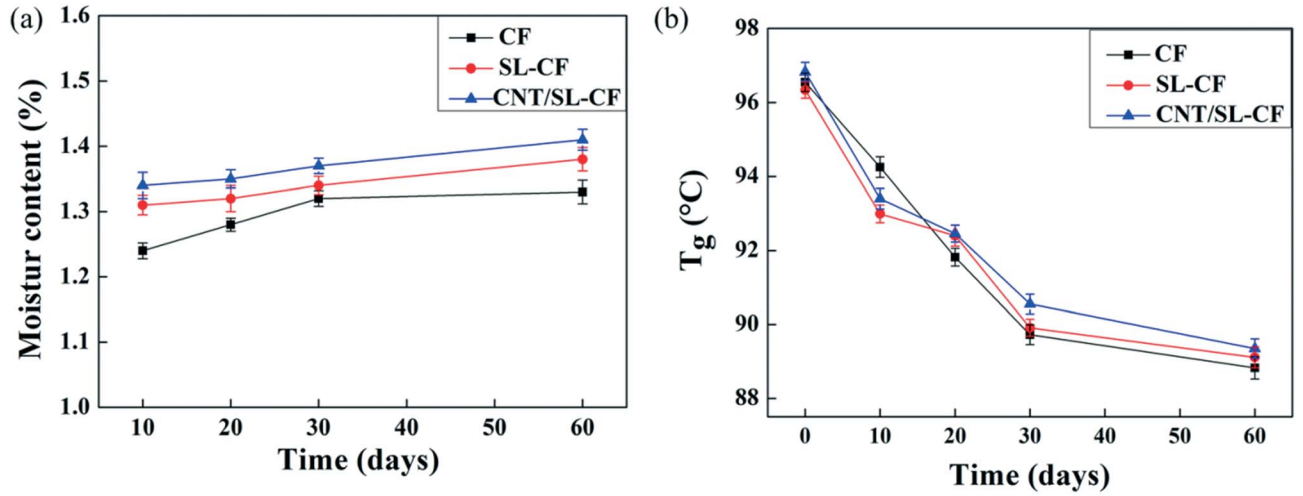

Fig. 2 (a) Percentage of weight increase of different CFRP composites immersed in water for certain days; (b) DMA results of different treated composites: CF, SL-CF and CNT/SL-CF.

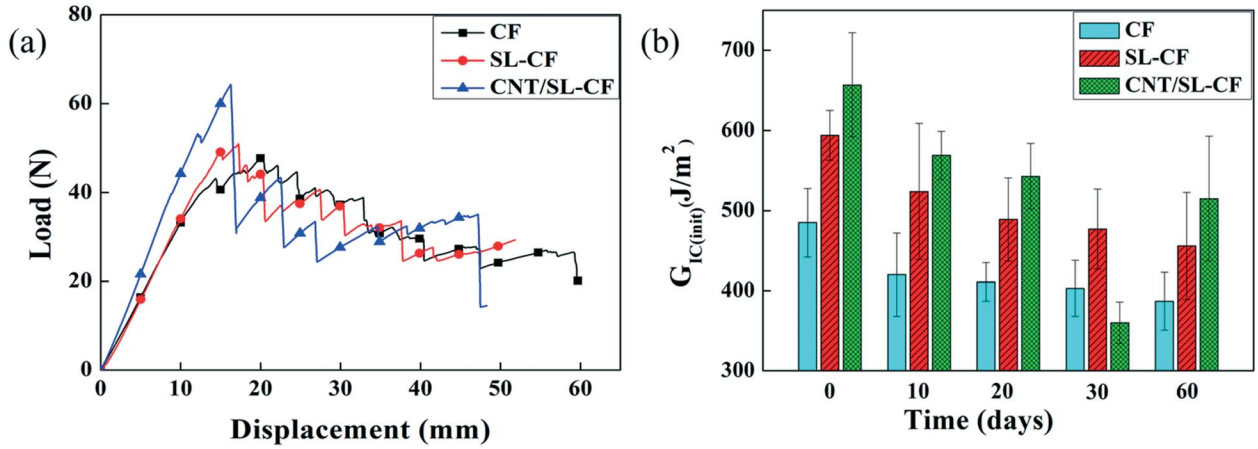

Fig. 3 (a) Typical load-displacement curves of Mode I interlaminar fracture toughness test; (b) $G_{IC(init)}$ of different CFRP composites immersed in water for certain days.

G_{IC} values of crack initiation for each treatment type are shown in Fig. 3b. The $G_{IC(init)}$ value shows an increase of 22.4% when carbon fibers are treated with silane and 35.4% when CNTs are incorporated into the silane coating. After a 60 days hygrothermal treatment, the $G_{IC(init)}$ of the SL-CF and CNT/SL-CF specimens are still 17.8% and 33% higher than the untreated ones. There is a strange decrease of $G_{IC(init)}$ after 30 days treatment for CNT/SL-CF treated specimens. It may be due to some technical mis-operations in sample preparation, which makes this datapoint unreliable. Fortunately, the rest data still clearly demonstrate the reinforced interlaminar fracture toughness of CNT/SL-CF during the hygrothermal aging. The increase of $G_{IC(init)}$ for silane treated CFRP composites is mainly due to the increased bonding strength between the fiber surface and the epoxy matrix. The silane coating can react with original sizing on carbon fibers on one side and form chemical bonding with epoxy matrix on the other side.[18] The CNT/SL-CF samples provide the highest $G_{IC(init)}$ and maintain high fracture toughness even after lengthy exposure to moisture. When CNTs are incorporated, thin layer of nanotube at the interface offers the opportunity for direct interaction both with the epoxy matrix and the carbon fiber when functional groups are available. Such interaction will directly affect interphase formulation of composites, and improve fracture toughness by CNTs bridging or CNTs pull-out.[18,25] In addition, CNTs act as interlocking pins and could increase the friction at the interphase area. The high stiffness of CNTs can also ameliorate the stress concentration and help stress transfer from fibers to matrix.

SEM micrographs of the fractured surfaces of the carbon fibers under different treatments are shown in Fig. 4. It can be seen that the CF samples have very smooth surface (Fig. 4a), while both the SL-CF and CNT/SL-CF samples show much rougher surfaces (Fig. 4c) and (Fig. 4e and g), respectively. The smooth surface of the CF samples implies that at point of failure, the matrix is broken away from the fibers due to poor adhesion, whereas the addition of both silane and CNTs improve the adhesive properties and so a considerable amount of matrix remains intact after delamination, resulting in higher fracture toughness values as a greater load is required to break the interfacial bonds for these samples. After 60 days exposure, the resin in the CF

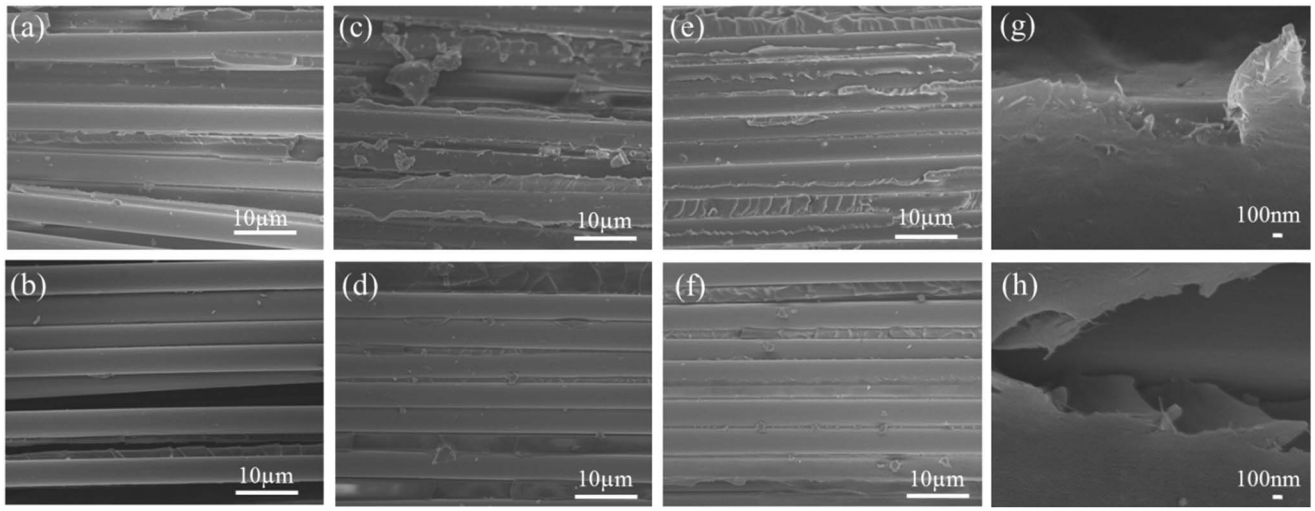

Fig. 4 SEM images of fractured surfaces of composites conditioned in water after DCB tests: (a) CF specimens before immersion; (b) CF specimens immersed for 120 days; (c) SL-CF specimens before immersion; (d) SL-CF specimens immersed for 120 days; (e) CNT/SL-CF specimens before immersion; (f) CNT/SL-CF specimens immersed for 120 days; (g) CNT/SL-CF specimens before immersion (high magnification); (h) CNT/SL-CF specimens immersed for 120 days (high magnification).

samples (Fig. 4b) and SL-CF samples (Fig. 4d) can be seen to have broken down and the CNT/ SL-CF samples (Fig. 4f and h) show weaker bonding between the matrix and fibers when being compared with dry samples, giving a smoother appearance in the SEM micrograph. So it can be confirmed that the presence of water aids in the deterioration of the interfacial properties and therefore the weakening of the composites.

3.4. Mode II interlaminar fracture toughness

The mode II fracture toughness was evaluated using Eq. (3) and Fig. 5a shows typical load-displacement curves for the three composite systems (CF, SL-CF, CNT/SL-CF). The average values of $G_{IIC(init)}$ for each treatment and water exposure interval are shown in Fig. 5b. There is a clear improvement seen in the mode II fracture toughness of the SL-CF and CNT/SL-CF samples. Before hygrothermal treatment, $G_{IIC(init)}$ of the SL-CF samples shows an improvement on the CF samples by 10.8%, whereas the $G_{IIC(init)}$ of the CNT/SL-CF samples is higher than the SL-CF samples by 19.9%. After being exposed in water for 60 days, the CNT/ SL-CF samples still show higher $G_{IIC(init)}$ even when compared with dried CF samples.

The fractured surfaces after ENF tests are shown in Fig. 6. The figures are similar to those of Mode I specimens. It can be seen that, before hygrothermal treatments, the CF samples have a relative smooth surface (Fig. 6a), while the other two kinds of samples show much rougher surfaces (Fig. 6c) and (Fig. 6e and g), respectively. After being immersed into hot water, the fractured surfaces of three types of composites all become smoother than before (as shown in Fig. 6b, d, f and h), which implies that hygrothermal treatments have negative effects on the interfacial bonding of CFRP. In Fig. 6g and h, CNTs can be clearly observed well dispersed on the surface of a carbon fiber; the matrix has been peeled away from the fiber but the process is somewhat resisted by the CNTs. These results imply the bonding strength is improved after surface treatments.

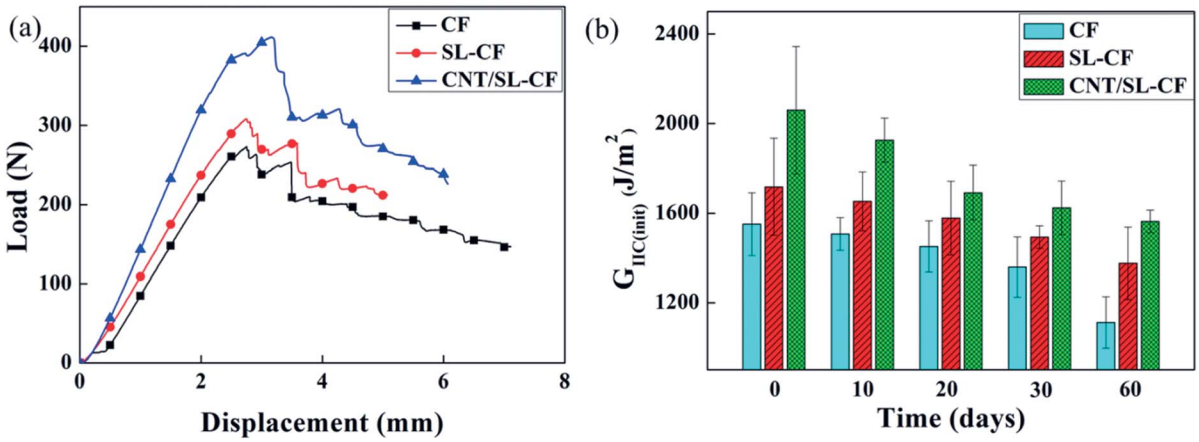

Fig. 5 (a) Typical load-displacement curves of Mode II interlaminar fracture toughness test; (b) $G_{IIC(init)}$ of different CFRP composites immersed in water for certain days.

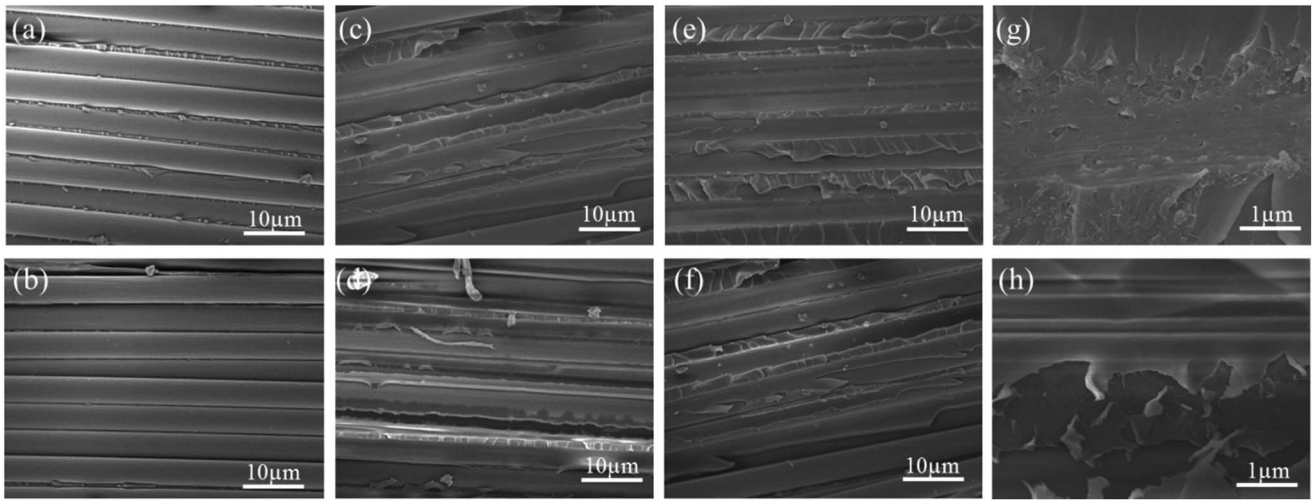

Fig. 6 Fracture surfaces of composites conditioned in water after ENF tests: (a) CF specimens before immersion; (b) CF specimens immersed for 120 days; (c) SL-CF specimens before immersion; (d) SL-CF specimens immersed for 120 days; (e) CNT/SL-CF specimens before immersion; (f) CNT/SL-CF specimens immersed for 120 days; (g) CNT/SL-CF specimens before immersion (high magnification); (h) CNT/SL-CF specimens immersed for 120 days (high magnification).

These images help to explain the interfacial interactions between the fiber and CNT despite the low CNT loading within the silane solution. The reinforcing and hygrothermal resistant mechanism of both silane and MWCNTs are similar with the Mode I fracture toughness tests as the above mentioned.

3.5. Interlaminar shear strength

The interlaminar shear strength of the samples was evaluated using Eq. (4) for each of the water exposure intervals, as shown in Fig. 7b. The SBS tests give accurate measures of the ILSS value only if pure interlaminar shear failures take place. Fig. 7a shows typical load-displacement curves for the three composite systems (CF, SL-CF, CNT/SL-CF). Fig. 8a shows an optical microscope image of a sample that has undergone interlaminar shear failure in the neutral plane due to maximum shear stress which is the ideal failure mode for the SBS samples. However, the specimen usually encounters other types of damage before or concurrent with interlaminar shear failure, causing the specimen to fail by other than pure interlaminar shear.[26–28] Fig. 8b shows a mixed failure mode, whereby the onset of cracking was initiated outside of the neutral plane and propagate at a 90° orientation. This type of failure mode yields unreliable results for ILSS tests, as other failure modes are dominant over interlaminar shear. Fig. 7a also shows a typical failed load-displacement curve of interlaminar shear strength test. Only if the load drops obviously immediately after the peak load is reached, it is assumed that the specimen failed in laminar shear.[26] Here in the tests, the peak load in this kind of circumstance was then used to determine the ILSS.

The ILSS decreased continuously with the duration of submersion in the water bath. The increase of ILSS for SL-CF specimens is not obvious compared with CNT/SL-CF specimens. That is because the shear failure strength is not only influenced by interfacial properties of CFRP but also largely dependent on pure matrix properties.[29] Silane can only improve interfacial bonding strength to some extent,

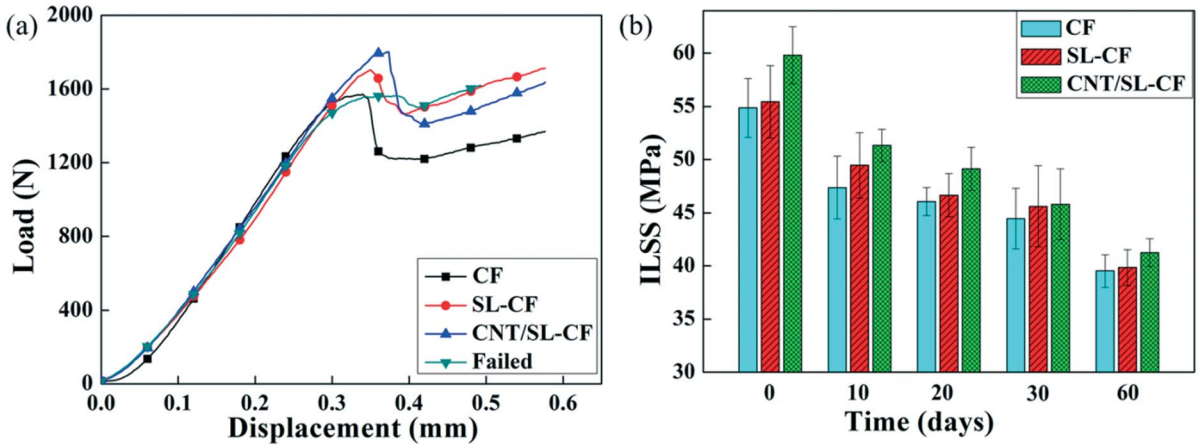

Fig. 7 (a) Typical load-displacement curves of Interlaminar shear strength test; (b) Interlaminar shear strength (ILSS) of different CFRP composites immersed in water for certain days.

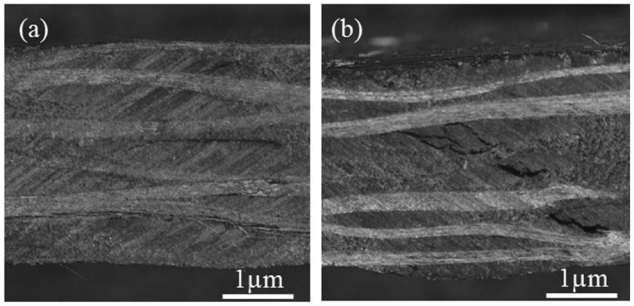

Fig. 8 Optical microscope images of different failure modes after SBS tests: (a) interlaminar shear failure mode; (b) mixed failure modes.

but not the epoxy matrix properties. So the effect of silane treatment is quite limited. However, the CNT/SL-CF composite system showed the best ILSS properties, which is 9% higher than CF specimens before hygrothermal treatments. After immersion in hot water, CNT/SL-CF samples still show a 4.3% higher ILSS than the untreated samples. It indicates that this treatment has beneficial effects on the ILSS. Three possible mechanisms of CNTs for shear strength enhancement seem to work.[25] Firstly, nanotubes act like rigid fillers, which can toughen and reinforce the epoxy matrix at the interphase area by serving as a crack arrester and prevent expansion of microcracking.[30] Secondly, nanotubes can improve the interfacial bonding strength of composites through the "bridging mechanism" in the resin-rich interphase area. In addition, the existence of CNTs can reduce the interlaminar stress concentration by smearing the mismatch of neighboring plies properties.

4. Conclusions

Hybrid CFRP composites have been prepared using the carbon fibers with MWCNT-doped silane coating. Effects of hygrothermal environment on mechanical properties of treated and untreated CFRPs have been characterized through mechanical tests and dynamic mechanical analysis. The experimental study reveals that there are two main reinforcing mechanisms in the hybrid composites: (i) The addition of the silane coupling agent generates an increase in all observed mechanical properties when being compared with CF samples. It has been established that the chemical bonding plays a significant role in this improvement, leading to an average increase in mode I and mode II fracture toughness by 22.4% and 10.8% compared with unmodified samples, respectively. The influence of silane surface treatment on the interlaminar shear stress is, however, not very significant due to this property is also affected by matrix properties. (ii) CNTs provide additional benefit by absorbing energy through their highly flexible elastic behavior during the deformation.[18,25] CNT/SL-CF composite shows a greater increase in all mechanical properties than composites treated with silane alone. The average mode I and II fracture toughness is improved by 35.4% and 32.8% compared with CF samples, respectively.

It has also been found that for each modification, exposure to water results in adverse effects on the ILSS, mode I and mode II fracture toughness, and glass transition temperature. These properties continually decrease with increasing exposure time. Surface treatments of carbon fibers can improve the hygrothermal resistance of hybrid CFRPs. CNT/SL-CF specimens still show the best performance after hygrothermal aging. The average mode I and II fracture toughness and interlaminar shear strength are improved by 33%, 40.5% and 4.3% compared with CF samples after 60-day immersion test, respectively. The increase is because the treatment reduces the likelihood of delamination and promotes uniform load transfer between matrix and fibers even under hygrothermal environment, thus increasing the durability of the composites. The improvements attained by this simple modification provides the great potential of silane and CNT modified composite laminates for large scale use in the marine industry.

5. Acknowledgments

The work is financially supported by the Materials Innovation for Marine and Offshore (MIMO) Program under the Agency for Science, Technology and Research (A*Star) of Singapore (Grant No. SERC1123004028), HKUST Start-up Fund (Grant No. R9365), and National Natural Science Foundation of China (Grant No. 11772131). We appreciate Hexcel to provide the free carbon fibers.

References

1 M. Li, H. Liu, Y. Gu, Y. Li and Z. Zhang, *Appl. Surf. Sci.*, 2014, **288**, 666–672.
2 S. Yumitori, D. Wang and F. R. Jones, *Composites*, 1994, **25**, 698–705.
3 F. Vautard, S. Ozcan and H. Meyer, *Composites Part A*, 2012, **43**, 1120–1133.
4 E. Pamula and P. G. Rouxhet, *Carbon*, 2003, **41**, 1905–1915.
5 S. Osbeck, R. H. Bradley, C. Liu, H. Idriss and S. Ward, *Carbon*, 2011, **49**, 4322–4330.
6 A. Godara, L. Gorbatikh, G. Kalinka, A. Warrier, O. Rochez, L. Mezzo, F. Luizi, A. W. van Vuure, S. V. Lomov and I. Verpoest, *Compos. Sci. Technol.*, 2010, **70**, 1346–1352.
7 T. Kamae and L. T. Drzal, *Composites Part A*, 2012, **43**, 1569–1577.
8 Y. Yang, C. X. Lu, X. L. Su and X. K. Wang, *J. Mater. Sci.*, 2007, **42**, 6347–6352.
9 X. Q. Zhang, X. Y. Fan, C. Yan, H. Z. Li, Y. D. Zhu, X. T. Li and L. P. Yu, *ACS Appl. Mater. Interfaces*, 2012, **4**, 1543–1552.
10 Y. I. Tsai, E. J. Bosze, E. Barjasteh and S. R. Nutt, *Compos. Sci. Technol.*, 2009, **69**, 432–437.
11 J. M. Zhou and J. P. Lucas, *Compos. Sci. Technol.*, 1995, **53**, 57–64.
12 F. Ellyin and R. Maser, *Compos. Sci. Technol.*, 2004, **64**, 1863–1874.
13 J. J. Imaz, J. L. Rodriguez, A. Rubio and I. Mondragon, *J. Mater. Sci. Lett.*, 1991, **10**, 662–665.
14 Y. Z. Wan, Y. L. Wang, Y. Huang, B. M. He and K. Y. Han, *Composites Part A*, 2005, **36**, 1102–1109.
15 H. L. Luo, J. J. Lian, Y. Z. Wan, Y. Huang, Y. L. Wang and H. J. Jiang, *Mater. Sci. Eng., A*, 2006, **425**, 70–77.
16 M. C. Lee and N. A. Peppas, *J. Appl. Polym. Sci.*, 1993, **47**, 1349–1359.
17 A. C. Loos and G. S. Springer, *J. Compos. Mater.*, 1979, **13**, 131–147.
18 B. Yu, Z. Jiang, X.-Z. Tang, C. Y. Yue and J. Yang, *Compos. Sci. Technol.*, 2014, **99**, 131–140.
19 S.-H. Lee, H. Kim, S. Hang and S.-K. Cheong, *Compos. Sci. Technol.*, 2012, **73**, 1–8.
20 G. Marom, in *Polymer permeability*, ed. J. Comyn, Elsevier, London, Ch. 9 edn., 1985.
21 G. M. Odegard and A. Bandyopadhyay, *J. Polym. Sci., Part B: Polym. Phys.*, 2011, **49**, 1695–1716.
22 P. C. Varelidis, N. P. Kominos and C. D. Papaspyrides, *Composites Part A*, 1998, **29**, 1489–1499.
23 A. Zafar, F. Bertocco, J. Schjodt-Thomsen and J. C. Rauhe, *Compos. Sci. Technol.*, 2012, **72**, 656–666.
24 C. Maggana and P. Pissis, *J. Polym. Sci., Part B: Polym. Phys.*, 1999, **37**, 1165–1182.
25 J. Zhu, A. Imam, R. Crane, K. Lozano, V. N. Khabashesku and E. V. Barrera, *Compos. Sci. Technol.*, 2007, **67**, 1509–1517.
26 Z. Fan, M. H. Santare and S. G. Advani, *Composites Part A*, 2008, **39**, 540–554.
27 F. Abali, A. Pora and K. Shivakumar, *J. Compos. Mater.*, 2003, **37**, 453–464.
28 W. C. Cui and M. R. Wisnom, *Compos. Sci. Technol.*, 1992, **45**, 323–334.
29 E. C. Botelho, L. C. Pardini and M. C. Rezende, *J. Mater. Sci.*, 2006, **41**, 7111–7118.
30 Y.Dzenis and D. Reneker, Delamination resistant composites prepared by small diameter fiber reinforcement at ply interfaces, *US Patent 6265333B1*, 2001.